



Concurrent high strength and high ductility in isotropic bulk Cu–Al alloy with three-dimensional nano-twinned structure

J.L. Ning*, D. Wang

Institute of Nanotechnology, Karlsruhe Institute of Technology, Hermann-von-Helmholtz-Platz 1, 76344 Eggenstein-Leopoldshafen, Germany

ARTICLE INFO

Article history:

Received 2 September 2011
Received in revised form
14 November 2011
Accepted 15 November 2011
Available online 23 November 2011

Keywords:

Cu–Al alloy
Nanostructure
Twinning
Ductility
Work hardening

ABSTRACT

A structure with extensive randomly oriented nanoscale deformation twins and twin intersections was introduced in a bulk Cu–Al alloy by multi-directional forging at room temperature. This three-dimensional nano-twinned structure led to isotropic mechanical properties with concurrent high strength and high ductility, attributed to enhancing the strain hardening rate. The strategy described here can be scaled up to produce large three-dimensional nanostructured materials for practical applications.

© 2011 Elsevier B.V. All rights reserved.

1. Introduction

To prepare engineering materials with both high strength and ductility has been a long-standing challenging issue for material scientists. Bulk ultrafine-grained (UFG) or nanostructured (NS) materials produced by severe plastic deformation (SPD) usually have high strength but relatively low ductility at ambient temperature [1–3]. This low ductility is attributed to the lack of strain hardening caused by their inability to accumulate dislocations because of their small grain sizes and saturation of dislocations [2–4]. Therefore, the basic idea to improve the ductility of UFG or NS materials is to enhance the strain hardening [3,5,6]. Recently, ductility was significantly enhanced with simultaneous high strength in single-phase metals or alloys by increasing strain hardening, attributed to the development of growth twins via pulsed electrodeposition [7–9] or deformation twins induced by various plastic deformation techniques [3,6,10,11]. Nanoscale growth twins in Cu via electrodeposition led to superior properties with both high strength and high ductility [7–9], but obtaining only foils or thin films by this method restricts its potential structural applications [3,11,12]. Bulk materials with nanoscale deformation twins can be fabricated by methods of plastic deformation, but some have also limitations on the scale of at least one dimension of the processed materials, such as rolling [3,6], high pressure torsion (HPT)

[6] and dynamic plastic deformation (DPD) [11,13,14]. Besides, the texture induced by deformation [3,6] or preferred orientation of deformation twins [11,13,15], especially a roughly monodirectional oriented twin bundles in large scale [11,13] can probably lead to anisotropic mechanical properties in the bulk materials. However, the anisotropy of the bulk materials with deformation twins is seldom studied to the authors' knowledge. Nevertheless, to produce large-scale bulk materials in three dimensions with isotropic properties of both high strength and high ductility is very attractive and meaningful for engineering applications. For this purpose, we employed an effective and economical method of multi-directional forging (MDF) to produce the large-scale three-dimensional bulk material, and reported the isotropic properties with both high strength and high ductility, which was attributed to the development of randomly oriented extensive nanoscale deformation twins and twin intersections (referred to as three-dimensional nano-twinned structure). The relationship between the mechanical properties and the microstructures was also investigated.

2. Experimental procedure

The material used in this study was a single phase Cu–6wt.%Al (Cu–13 at.%Al) alloy with a stacking fault energy (SFE) of $\sim 6 \text{ mJ m}^{-2}$ [16]. Before plastic deformation, the alloy was annealed in vacuum at 800 °C for 1 h to obtain a homogeneous microstructure with a grain size in the range of 300–400 μm . The rectangular sample with dimensions of 7.5 mm \times 7.5 mm \times 5.5 mm was subjected to MDF at a strain rate of about $5 \times 10^{-3} \text{ s}^{-1}$ at room temperature (RT). The equivalent strain of each pass was 0.3, which is defined as $\epsilon_{\text{eq}} = (2/\sqrt{3}) \ln(L_0/L_f)$, where L_0 and L_f are the heights in the loading direction before and after each pass, respectively. The loading direction was changed sequentially along the three orthogonal axes of the

* Corresponding author. Tel.: +49 0176 77378689.

E-mail addresses: jiangli.ning@kit.edu, jianglining.cn@gmail.com (J.L. Ning).

rectangular sample from pass to pass. Finally an accumulative equivalent strain of 1.8 was obtained after six sequential passes, and consequently the dimensional ratio of the rectangular sample was almost unchanged. No flaws (cracks or porosities) were detected inside the deformed sample.

Microstructure characterization was performed on an optical microscope (OM, Zeiss Axiotech) and a FEI Titan 80-300 transmission electron microscope (TEM) operated at 300 kV. The observations were carried out on the sections perpendicular to the three orthogonal loading axes of the MDF sample. For OM observations, the samples were etched in a solution containing HNO_3 , H_3PO_4 and $\text{C}_2\text{H}_4\text{O}_2$ (with a ratio of 1:2:1). The TEM foils were prepared by mechanical grinding, followed by thinning via double-jet electropolishing. Microhardness (HV) was also measured on the sections perpendicular to the three orthogonal axes, using a Buehler microindenter at a load of 2N. At least seven indents were measured for each section. Uniaxial tensile tests were performed on a dedicated tensile machine for miniature specimens at a strain rate of $5 \times 10^{-4} \text{ s}^{-1}$ at ambient temperature. A contactless laser extensometer (Fiedler Optoelectronics P-50) was used to precisely measure the sample strain upon loading. Dog-bone-shaped tensile specimens were cut into a gauge length of 2 mm, with a width of 1 mm and a thickness of 0.3 mm, from the MDF sample along two of the three orthogonal loading axes. At least two tensile samples were tested along the same loading axis to substantiate the reproducibility of the stress–strain curves.

3. Results

The optical observations on the three orthogonal sections from the MDF sample indicated similar microstructural features. High density of deformation markings as parallel lines were visible in every original coarse grain, with the lengths in a range of several micrometers, as seen in Fig. 1(a), which were verified to be bundles of deformation twins by further TEM observations. The correspondence between the observed deformation markings in optical microstructure and the twin bundles in TEM microstructure was also reported in [13,15–17]. The twin bundles were not straight but curved, typical characteristics of deformation twins [10,11]. The orientations of deformation twins were random in the original grains and distinct with each other. A grain orientation dependence of deformation twinning was identified in coarse-grained Cu subjected to dynamic plastic deformation, explained in terms of Schmid factor analysis [18]. According to [18], it can be postulated that the alternative loading direction during MDF facilitated deformation twins occurring in every grain with original random orientations.

Almost in each original grain deformed by MDF, intersections of deformation markings were observed, as seen in Fig. 1(b). These intersecting deformation markings were verified to be intersections of deformation twins by TEM. The high frequency of the intersections, which can be estimated as the fraction of original grains containing twin intersections after MDF, was almost 100%. It will essentially influence the mechanical properties of the alloy.

Finer microstructures were characterized by TEM, and showed similar features from the three orthogonal sections of the MDF sample. The TEM image of lower magnification in Fig. 2(a) shows that high density of deformation twins have formed in the deformed sample, corresponding with the observations by optical microscope. The TEM image of higher magnification and the corresponding selected area electron diffraction (SAED) pattern in Fig. 2(b) show the typical features of deformation twins. Nanoscale twin/matrix (T/M) lamellae formed the twin bundles, as seen in Fig. 2(b), the corresponding SAED pattern exhibited a superposition of a couple of $\langle 011 \rangle$ diffraction patterns which were symmetrical to each other with respect to the $\{111\}$ plane, indicating a typical twin relationship of face-centered cubic (fcc) metals. Most twin boundaries (TBs) were curved, typical characteristics of deformation twins, which may originate from the fact that a high density of dislocations existed at the boundaries of twins [11]. The high density of dislocations at TBs is a typical feature of deformation-induced twins [3,6,10,11,13], which implies a large stress concentration in the T/M lamellae, as indicated by the contrast in Fig. 2(b).

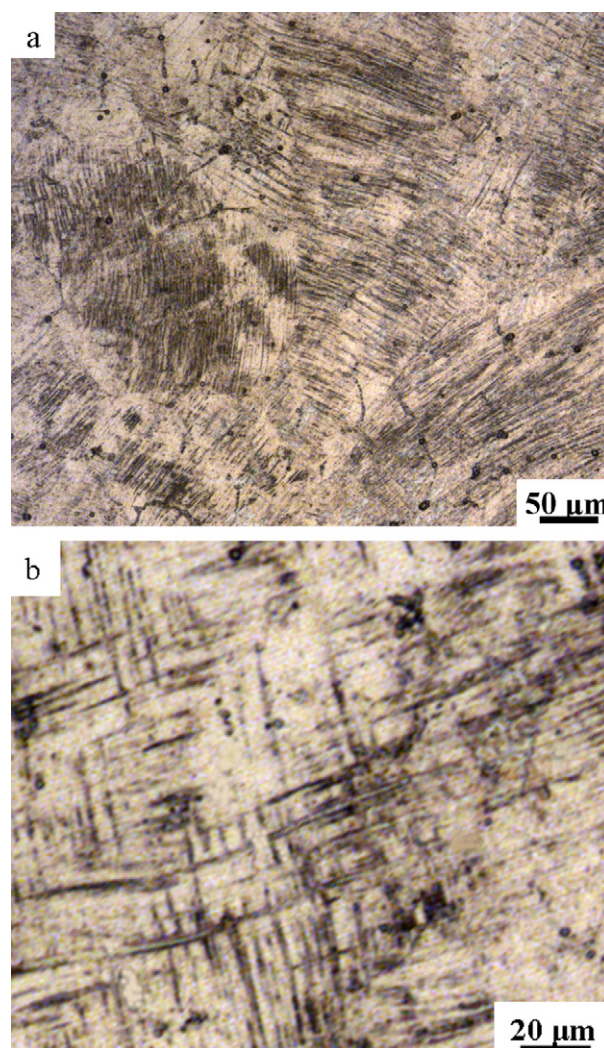


Fig. 1. Typical optical micrographs on one section from the MDF sample showing: (a) high density of deformation markings as parallel lines; (b) intersections of deformation markings.

Statistical measurements of the T/M lamellar thickness from many TEM images in different regions indicated that the thickness was distributed in a range of several nm to ~ 110 nm, as shown in Fig. 2(c). The thickness of most lamellae varied from a few nanometers to 40 nm, with an average value of about 24 nm, which indicated that the present MDF was efficient to induce high density nanoscale T/M lamellae in this Cu–Al alloy.

TEM micrograph of a large area in Fig. 3(a) shows high frequency of twin–twin intersections existing in the MDF sample, which is consistent with the observations by optical microscope. The occurrence of twin–twin intersections indicated that different twinning systems were activated in the sample during the shear deformation [10,19,20]. Closer observation by TEM in the region with intersections of deformation twins, as shown in Fig. 3(b), revealed the typical characteristics of intersecting deformation twins, in which it can be seen that two sets of twin bundles intersected at a large angle close to 90° , resulting in nanoscale rhombic blocks [10,15,19,20]. Twin–twin intersections were frequently observed in fcc materials with low SFEs, such as Cu alloys [10,15,19], stainless steels [20]. When the driving force for deformation twinning is large enough to overcome the barriers of the encountered TBs, intersections of twins on different planes take place [21]. Several factors can facilitate the occurrence of twin–twin intersections: (1) a large strain and high strain rate (e.g. 10^3 – 10^4 s^{-1}) may activate a high density

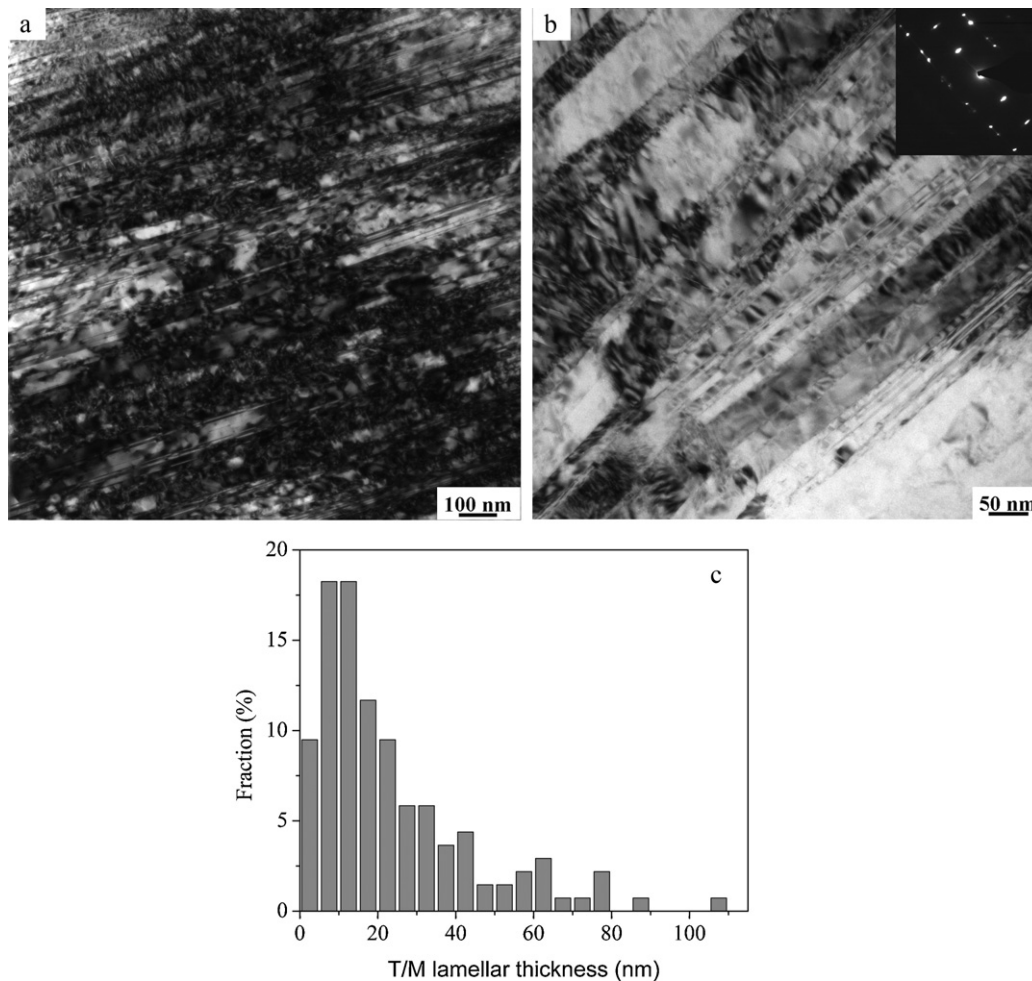


Fig. 2. (a and b) Typical bright-field TEM images from one section of the MDF sample: (a) image of lower magnification showing the high density of deformation twins; (b) image of higher magnification showing nanoscale T/M lamellae and the corresponding SAED pattern; (c) statistical T/M lamellar thickness distribution determined from numerous TEM images.

of multisystem deformation twins to accommodate the straining; (2) a multidirectional repetitive loading may facilitate formation of different twin systems, leading to deformation twins intersecting not only with the current cooperative twin systems, but also with the previously generated twins [20]. The high frequency of twin intersections in the present Cu–Al alloy indicated that MDF was very efficient to induce this structure even processed at a low strain rate, which can be attributed to the specific deformation feature of multidirectional repetitive loading, facilitating to activate different twinning systems.

It is well known that TBs are typically coherent boundaries with low excess energies, which are particularly simple case of periodic boundaries or special high-angle boundaries (HABs) with a very high degree of coincidence, i.e., $\Sigma 3$ or $\Sigma 9$ coincident-site lattice (CSL) boundaries [3,7,8,20,22,23]. Parallel twins in one direction (twin bundles) result in lamellar twin–matrix alternative blocks separated by TBs. When two sets of deformation twins are activated to accommodate the deformation, twin–twin intersection will be inevitable to produce rhombic blocks, and other shaped blocks with different sets of twin intersections [20,21], as shown in Fig. 3(a) and (b). Previously developed mechanisms [20,24] interpreting the twin–twin intersections implied that the intersections produced rhombic blocks with changed orientations and bordered by special HABs ($\Sigma 3$ and $\Sigma 9$ etc.). These boundaries are quite different from the dislocation boundaries usually developed in the plastic deformed materials with medium–high SFEs, and need not

absorption of accommodation dislocations to increase their boundary misorientations [20,22].

Fig. 4(a) shows the microhardness values measured on the three orthogonal sections. The HV values varied in a narrow range on each of the three sections with the standard deviations of 4, 4 and 6, respectively. Since the indents were uniformly distributed on the surface of each section, it implied that the deformation-induced microstructure was quite homogeneous on each section. The ranges of the HV values on the three sections overlapped to a large extent with each other, indicating that the three orthogonal sections had an approximately same range of microhardness value, with the average HV values of 194, 199 and 189, respectively. It implied that there was no deformation-induced anisotropy in the MDF sample, which was coincident with the microstructure observations by OM and TEM.

Fig. 4(b) illustrates two typical tensile stress–strain curves with the gauge lengths along two of the orthogonal loading axes of the MDF sample, which indicates very similar deformation behaviors with coincident flow curves, and both exhibit similar remarkable strain hardening stages. The tensile tests along the two orthogonal axes showed equivalent value ranges of strength and ductility, presenting values as 0.2% yield strength (YS) of 690 ± 25 MPa, ultimate strength (UTS) of 785 ± 25 MPa, uniform elongation (UE) of $3.5 \pm 0.35\%$ and elongation to failure of $20.7 \pm 1.3\%$. The UE was determined using the Considère criterion [3,6,25]. The tensile tests as well as the microhardness measurements along the different

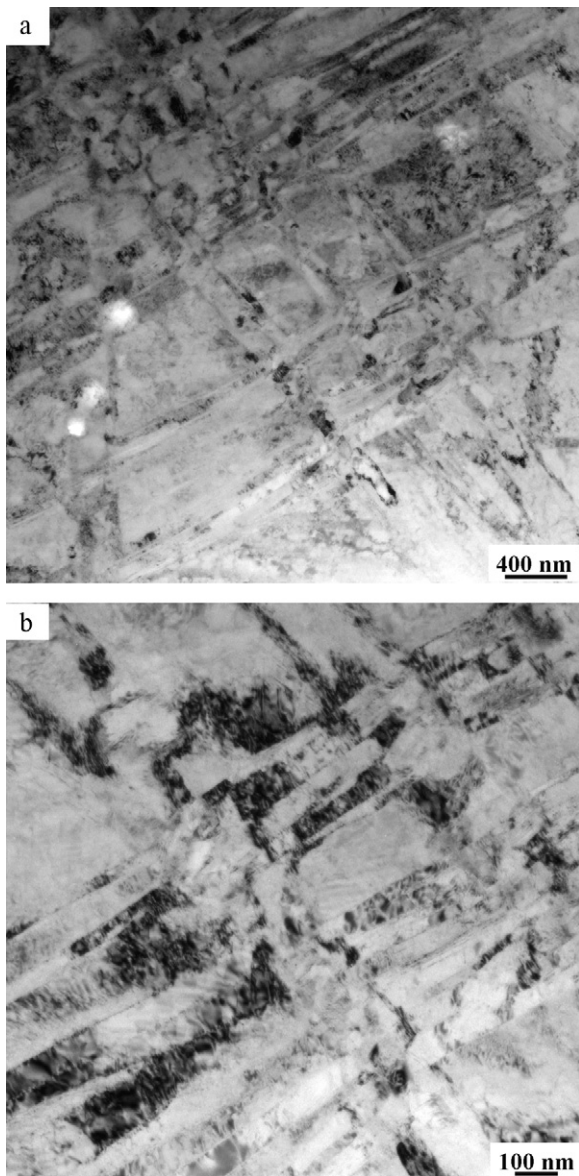


Fig. 3. Typical bright-field TEM images from the region with intersecting deformation twins: (a) an observation of a large area; (b) a close observation of the twin–twin intersections.

orthogonal directions demonstrated isotropic mechanical properties in the MDF sample, which was attributed to the homogeneous distribution of the randomly oriented twin bundles and twin–twin intersections. Therefore, the present MDF showed a merit to obtain homogeneous, isotropic bulk NS materials, without limitation on the scale of all the three dimensions of the billet, and thus had a potential to be scaled up to process large bulk materials for various applications.

4. Discussion

Lots of researches [3,6–12,14,23] have revealed that generation of nanoscale twins, i.e., growth twins or deformation twins, in metals and alloys can offer substantial strengthening while preserving acceptable levels of ductility. The strengthening of TBs was described to be quantitatively identical to that of ordinary grain boundaries (GBs), and the trend of increasing strength with decreasing twin lamellar thickness was able to be explained by the Hall–Petch relationship, because the TBs serve as effective barriers

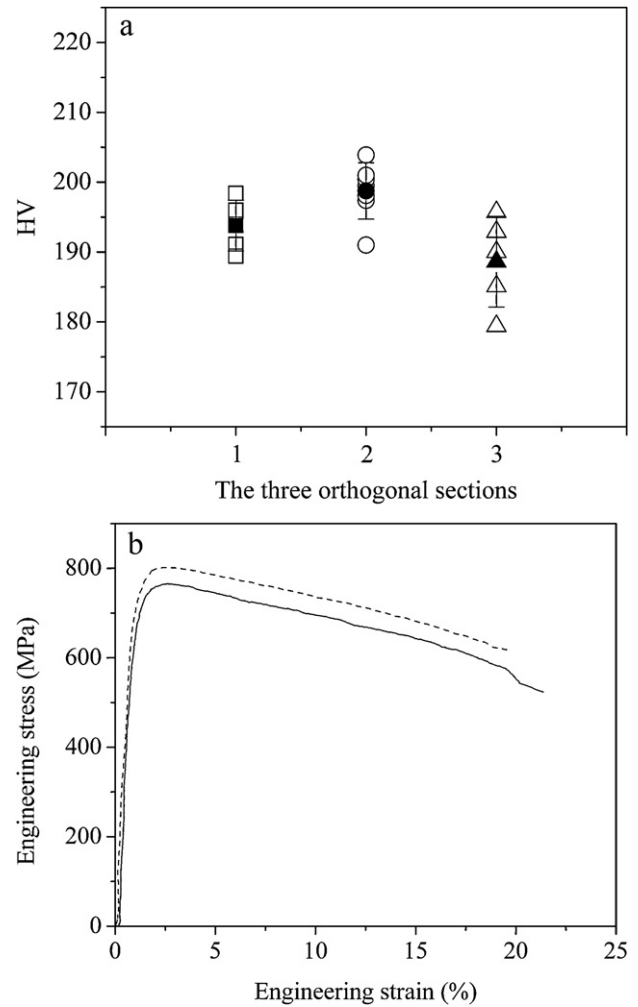


Fig. 4. (a) The microhardness values measured on the three orthogonal sections of the MDF sample; (b) the two typical tensile engineering stress–strain curves with the gauge lengths along two of the orthogonal loading axes of the MDF sample.

to dislocation motion for strengthening, like GBs [7,9,12,23]. Specifically, unlike in conventional grain refinement, the strengthening by nanoscale TBs is not accompanied by a sharp reduction in ductility, which is ascribed to the extraordinary work hardening capability and rate of nano-twinned structure, because of its rendering ample room for the storage and accumulation of additional defects (dislocations) [3,6–12,23]. The origin of the large capacity for, and the fast rate of, dislocation storage was attributed to the following factors. First, the twin lamellar structure may be viewed as “inherently bimodal”, because the length scale in the two dimensions parallel to the TBs is significantly larger than the nanoscale in the direction perpendicular to TBs. Dislocations can thus accumulate, forming tangles to subdivide the twin lamellae [8]. Second, nanoscale TBs creates more local sites for nucleating and accommodating dislocations, which originate from the dislocation–TB interactions that differ fundamentally from the dislocation–GB interactions in nano-grained and coarse-grained metals [23]. The density of accumulated partial dislocations at TBs estimated from TEM observations of deformed nano-twinned Cu can be two orders of magnitude higher than that of lattice dislocations stored in coarse-grained Cu and much higher than that in the nano-grained Cu [23]. Simultaneously, the interactions between dislocations and TBs are accompanied by a gradual loss of coherency of the TBs [8,23]. Meanwhile, it should be noticed that although deformation twins were indicated to be not fully coherent as growth twins, of

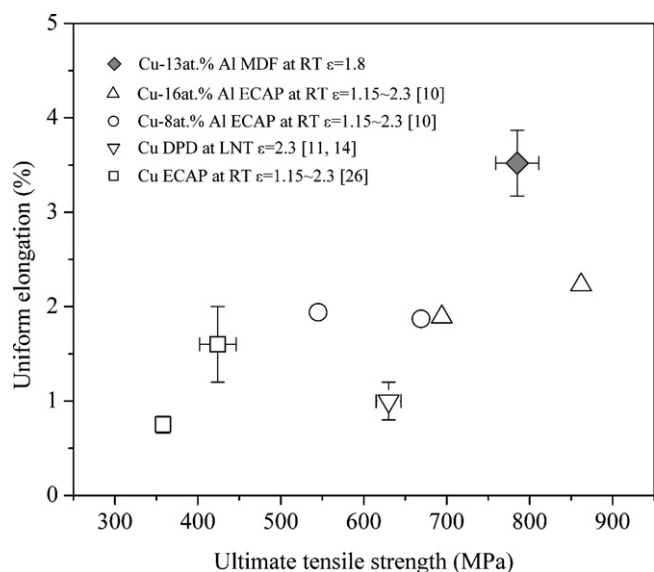


Fig. 5. The comparison of the tensile properties (UTS and UE) between the present Cu–13 at.%Al alloy processed by MDF and the data of Cu and various Cu–Al alloys deformed by different techniques to comparable equivalent strains from literatures [10,11,14,26].

which the excess energy is relatively higher, as a high density of partial dislocations already exist along deformation TBs [3,6,11,23], but plenty of researches have showed that deformation-induced nano-twinned structures are also very effective on strengthening and enhancing work hardening rate, and hence ameliorating ductility (though the effect can be weaker than the growth twins with perfect TBs, but they still exhibit more superior properties than conventional GBs) [3,6,10,11,14,22]. In addition, it was pointed out that the formation of extensive twin–twin intersections promoted higher work hardening rate, compared with the parallel twin lamellae in one direction (primary twins) [10,15]. The extensive intersecting twins formed in a grain will inhibit slip on essentially all slip systems, unlike the primary twins that only affect the non-coplanar slip systems, and will be propitious to the further enhancement of the work hardening rate [10,15].

The tensile properties of the present Cu–13 at.%Al alloy processed via MDF indicated a good combination of high strength and high ductility. Fig. 5 shows the comparisons of the tensile properties between the present data and the data from literatures, which are properties of Cu and Cu–Al alloys processed by different deformation methods to comparable equivalent strains with the present MDF. The data of Cu processed by equal channel angular pressing (ECAP) for 1–2 passes (equivalent strain of ~ 1.15 to ~ 2.3) at room temperature (RT) [26] showed a lowest combination of strength and ductility, which was attributed to the dominated microstructure of lamellar dislocation boundaries with low misorientation angles. The common microstructural features of high density TBs in the present MDF alloy and the others in Fig. 5 provided higher strain hardening rate [3,6–12], leading to both high UTS and high UE. The Cu processed by DPD at liquid nitrogen temperature (LNT) to a strain of 2.3 [11] presented a comparable average T/M lamellar thickness of ~ 40 nm with the present MDF alloy, but UTS and UE of the LNT-DPD Cu were still much lower than the present data. Besides the reason lack of the solution hardening of Al element and the higher SFE, the approximate one to two magnitude higher density of dislocations ($10^{15}\text{--}10^{16}\text{ m}^{-2}$) induced by the cryogenic deformation limited the capability of strain hardening. Additionally, because of the two-dimensional twin lamellae with TBs roughly parallel with the tensile loading direction, the GBs strengthening effect could be neglected in the LNT-DPD Cu.

In contrast, the randomly oriented twin bundles and twin intersections in the MDF alloy, which can be referred to as a structure of three-dimensional extensive deformation twins, provided more effective blockage of dislocation slip and more dislocation accumulation sites, thereby leading to a higher strain hardening rate, and consequently higher UE and UTS.

A previous study on Cu–Al alloys processed by ECAP at room temperature [10] indicated that decreasing SFE by adding Al element led to a simultaneous increasing of strength and uniform ductility, which was attributed to the extensive deformation twins and twin intersections induced by ECAP deformation. The UTS of the present Cu–13 at.%Al deformed by MDF was between those of the Cu–16 at.%Al processed by ECAP for one and two passes, which was corresponding to the comparable equivalent strains and similar Al contents. But the UE of the MDF alloy (3.5%) was obviously higher than the highest data (2.23%) reported in [10]. This was probably attributed to the higher frequency of twin intersections in the present MDF alloy, with a 100% fraction of original grains containing extensive twin intersections, facilitated by the specific deformation feature of MDF. Apparently, the high-density three-dimensional nano-twinned structure induced by the MDF exhibited mechanical properties with both high strength and good ductility.

Moreover, it is well known that to obtain extensive deformation twins in metals or alloys several factors are required, such as lowering the SFEs of alloys, or deforming at high strain rates and/or at low deformation temperatures [3,6,10,11,27]. However, it is difficult to enhance the strain rate or lower the deformation temperature to a large extent in some deformation methods, ex. ECAP, though it is also suitable for processing large-scale bulk materials, but to obtain microstructure with extensive deformation twins and twin intersections there is a limitation in selecting the materials concerning SFEs [10,28]. By contrast, MDF has an advantage to process materials at a wide range of strain rates and deformation temperatures, and thereby it provides a possibility to obtain extensive deformation twins and twin intersections in materials with a wide range of SFEs, and superior properties with both high strength and high ductility can be expected.

5. Conclusions

An isotropic bulk Cu–Al alloy with three-dimensional extensive deformation twins was obtained successfully by MDF, the microstructures and mechanical properties were identical in the three orthogonal directions of the processed billet. A concurrent high strength and high ductility was induced by introducing extensive deformation twins and twin intersections via enhancing the strain hardening rate. Furthermore, if the processing parameters and the alloying concerning SFE are optimized, the strength and ductility can possibly be enhanced to rather higher levels and result in superior properties. Due to the easiness and economical efficiency of the MDF process, the strategy described here can be readily scaled up to process large three-dimensional bulk NS materials for practical applications.

Acknowledgements

The authors would like to acknowledge Prof. Dr. Jixiang Fang for providing materials and samples, in addition of the assistance on experiments.

References

- [1] R.Z. Valiev, R.K. Islamgaliev, I.V. Alexandrov, Prog. Mater. Sci. 45 (2000) 103–189.
- [2] D. Jia, Y.M. Wang, K.T. Ramesh, E. Ma, Y.T. Zhu, R.Z. Valiev, Appl. Phys. Lett. 79 (2001) 611–613.

- [3] Y. Zhao, J.F. Bingert, X. Liao, B. Cui, K. Han, A.V. Sergueeva, A.K. Mukherjee, R.Z. Valiev, T.G. Langdon, Y.T. Zhu, *Adv. Mater.* 18 (2006) 2949–2953.
- [4] Y.T. Zhu, X.Z. Liao, *Nat. Mater.* 3 (2004) 351–352.
- [5] Y. Wang, M. Chen, F. Zhou, E. Ma, *Nature* 419 (2002) 912–915.
- [6] Y.H. Zhao, Y.T. Zhu, X.Z. Liao, Z. Horita, T.G. Langdon, *Appl. Phys. Lett.* 89 (2006) 121906.
- [7] L. Lu, X. Chen, X. Huang, K. Lu, *Science* 323 (2009) 607–610.
- [8] E. Ma, Y.M. Wang, Q.H. Lu, M.L. Sui, L. Lu, K. Lu, *Appl. Phys. Lett.* 85 (2004) 4932–4934.
- [9] X.H. Chen, L. Lu, K. Lu, *Scripta Mater.* 64 (2011) 311–314.
- [10] S. Qu, X.H. An, H.J. Yang, C.X. Huang, G. Yang, Q.S. Zang, Z.G. Wang, S.D. Wu, Z.F. Zhang, *Acta Mater.* 57 (2009) 1586–1601.
- [11] W.S. Zhao, N.R. Tao, J.Y. Guo, Q.H. Lu, K. Lu, *Scripta Mater.* 53 (2005) 745–749.
- [12] Y.F. Shen, L. Lu, Q.H. Lu, Z.H. Jin, K. Lu, *Scripta Mater.* 52 (2005) 989–994.
- [13] Y.S. Li, N.R. Tao, K. Lu, *Acta Mater.* 56 (2008) 230–241.
- [14] Y.S. Li, Y. Zhang, N.R. Tao, K. Lu, *Scripta Mater.* 59 (2008) 475–478.
- [15] S. Asgari, E. El-Danaf, S.R. Kalidindi, R.D. Doherty, *Metall. Mater. Trans.* 28A (1997) 1781–1795.
- [16] A. Rohatgi, K.S. Vecchio, G.T. Gray III, *Metall. Mater. Trans.* 32A (2001) 135–145.
- [17] A. Rohatgi, K.S. Vecchio, G.T. Gray III, *Acta Mater.* 49 (2001) 427–438.
- [18] C.S. Hong, N.R. Tao, K. Lu, X. Huang, *Scripta Mater.* 61 (2009) 289–292.
- [19] X. An, Q. Lin, S. Qu, G. Tang, S. Wu, Z.F. Zhang, *J. Mater. Res.* 24 (2009) 3636–3646.
- [20] H.W. Zhang, Z.K. Hei, G. Liu, J. Lu, K. Lu, *Acta Mater.* 51 (2003) 1871–1881.
- [21] N.R. Tao, K. Lu, *Scripta Mater.* 60 (2009) 1039–1043.
- [22] Y. Zhao, T. Topping, J.F. Bingert, J.J. Thornton, A.M. Danglewicz, Y. Li, W. Liu, Y. Zhu, Y. Zhou, E.J. Lavernia, *Adv. Mater.* 20 (2008) 3028–3033.
- [23] K. Lu, L. Lu, S. Suresh, *Science* 324 (2009) 349–352.
- [24] R.W. Armstrong, *Science* 162 (1968) 799–800.
- [25] S.K. Panigrahi, R. Jayaganthan, *J. Alloys Compd.* 509 (2011) 9609–9616.
- [26] F.D. Torre, R. Lapovok, J. Sandlin, P.F. Thomson, C.H.J. Davies, E.V. Pereloma, *Acta Mater.* 52 (2004) 4819–4832.
- [27] Z. Zhang, M. Wang, Z. Li, N. Jiang, S. Hao, J. Gong, H. Hu, J. *Alloys Compd.* 509 (2011) 5571–5580.
- [28] C.M. Cepeda-Jiménez, J.M. García-Infanta, O.A. Ruano, F. Carreño, *J. Alloys Compd.* 509 (2011) 9589–9597.